Development of a liquefied biomass electrocracking process – Application to biorefinery

Ana Priscila Resina de Almeida Ferreira

Chemical Engineering Department, Instituto Superior Técnico, Av. Rovisco Pais, 1, 1049-001 Lisbon, Portugal

Abstract

Biomass has been used mainly through direct combustion as a source of renewable energy. Liquefaction of biomass is an effective thermochemical process for the conversion of lignocellulosic matter into liquid products (bio-oil). A recent concept (electrocracking) has been developed due to the high amount of hydrocarbons in biomass. Electrocracking consists of the decomposition of organic compounds into value-added ones through electrolysis and the consequent production of H_2. Thus, this study focused on the development of a liquefied biomass electrolyser, exploring the hydrogen evolution reaction at the cathode and the production of new compounds at the anode. Also, the incorporation of aqueous solutions from the liquefaction process (from the condensation of vapours produced during liquefaction reaction and the water collected during liquid-liquid extraction of the biofuel obtained from the liquefaction of biomass) on the electrolyte solution has been studied in order to decrease waste in the industry. Beyond this, one of the renewable energy-based solutions found for the decarbonisation of industries is the incorporation of CO_2 in electrolysis and the production of added-value compounds. Thus, this work focused on the study and optimisation of electrolysis of liquefied biomass (from Secil Group) adding a 2 M KOH solution and water from the liquefaction process. Several electrochemical studies were carried out, involving the use of cyclic voltammetry, linear scan voltammetry, and rotating disc and ring-disc electrode techniques. Electrolysis tests were carried out on a laboratory electrolyser changing some of the operation variables, such as the temperature, anode material, type of current, cell voltage, and the effect of CO_2 bubbling. The tests that generated a higher amount of gas were the ones using Ni electrodes, direct current at 70 ºC, and alternating current at room temperature. The experiment with direct current (70 ºC) produced 55 mL of gas with 43% Faradaic efficiency and 39 % energetic efficiency, respectively. The alternating current experiment generated 102 mL of gas with 30 % Faradaic efficiency and 11 % energetic efficiency, respectively. The FTIR analysis did not reveal changes in the functional groups of the electrolyte solution before and after electrolysis. Lastly, the ash content of the solid deposited at the anode was quantified to be 36 %.

Keywords: Liquefied biomass; Electrolysis; Hydrogen; CO_2 reduction.

1 Introduction

The term biomass is used for all organic matter from plants. Biomass is produced from green plants that transform solar light in plant material through photosynthesis [1]. Lignocellulosic biomass is the most abundant plant material, therefore available in high quantities at a low cost [2]. However, when biomass is used as raw material is very important to implement a reforestation program, as it is not an endless power source [1] Biomass is used to overcome different energetic needs, such as electricity generation, domestic heat, fuel for vehicles and heat for industries. However, mainly it is used through direct combustion [3]. The process of liquefaction of biomass has been introduced as an effective thermochemical process to transform lignocellulosic biomass in liquid products using a solvent [4]. One of the main purposes of liquefaction is to reduce the oxygen content of biomass as it represents 40-50 wt.% of biomass [5]. The resulting bio-oil has a complex composition with a wide variety of oxygenated compounds, such as acetic acid, ethanol, carboxylic acids, phenols, aldehydes, ketones, alcohols, and esters [3]. Therefore, bio-oil can be used as biofuel, to produce bio-polyols, antioxidants and chemical compounds derived from hydrocarbons and lignin [6].

Hydrogen has been considered as a clean fuel for the future and in addition, its energy density is about 2.75 times bigger than other hydrocarbon fuels [3]. The designation of the clean nature of this fuel comes from the fact that its combustion generates only water. So, as an energy source has the advantages of low levels of pollution and a variety of applications [3,7]. One of the most promising technologies to produce H_2 is electrolysis [7]. Electrolysis of water powered by renewable energy has been extensively studied because it has the potential to enable hydrogen production scale-up. This process induces the dissociation of water into hydrogen and oxygen under the influence of an electric current [8]. Additionally, from all the existing CO_2 capture technologies, the one that

has recently aroused the most interest is the CO_2 electrochemical reduction reaction [9]. This process can capture CO_2 and consequently produce added-value products, such as carbon monoxide (CO), formic acid (HCOOH), formaldehyde (HCHO), and methane (CH_4) [10].
Recent research has introduced a new concept that interconnects electrolysis (with hydrogen production) with liquefied biomass, denominated electrocracking. This concept consists of the decomposition of the organic compounds from liquefied biomass into lighter hydrocarbons through the passage of current between two electrodes [11].
Herein, the incorporation of liquefied biomass from the liquefaction process made by Secil Group (as well as water from the liquefaction process) and CO_2 capture in electrolysis was investigated. Electrolysis tests were carried out on a laboratory electrolyser changing some of the operation variables, such as the temperature, anode material, type of current, cell voltage, and the effect of CO_2 bubbling. Also, several electrochemical fundamental studies were carried out. These included cyclic voltammetry and linear scan voltammetry.

2 Experimental

2.1 Electrolyte preparation and characterisation

In this study, it was used an emulsion composed of liquefied biomass and a 2 M KOH aqueous solution (50 vol.%). Additional tests were made using aqueous solutions from two distinct phases of the liquefaction process (from the condensation of vapours produced during the liquefaction reaction and the water collected during the liquid-liquid extraction of the biofuel obtained from the liquefaction of biomass). The aqueous phases coming from the liquid-liquid extraction (two-phase aqueous solution) were named dark phase and light phase.
For both electrolytes, the values of conductivity (σ), pH and were registered. Specifically, for the emulsion (liquefied biomass + KOH (2 M)) was measured the density (ρ) and was made a humidity content test using a VWR (IT 1400108) balance. For conductivity and pH measures was used a HANNA Instruments (pH20) device and for density was used a pycnometer.

2.2 Electrochemical measurements

Cyclic voltammetry (CV), RDE/RRDE, and linear scan voltammetry (LSV) tests were run using a bipotentiostat ALS 2325 in a 60 mL electrolytic cell with a jacket. The first two tests were carried out using a typical three-electrode arrangement, comprising a platinum (Pt) mesh (A = 50 cm^2) as the counter electrode, a saturated calomel electrode (SCE) as the reference electrode, and a Pt disc (A = 0.1256 cm^2) as the working electrode. Particularly, for RRDE tests both the disc and the ring were made of Pt (A_{disc} = 0.1256 cm^2, A_{ring} = 0.1885 cm^2). For LSV tests, the difference relied on the working electrode. In these tests, it was used a Pt electrode with an area of 1 cm^{-2} and a nickel (Ni) electrode (A = 22.4 cm^2)
For the CVs, a potential scan between the open circuit potential (OCP) and 0.6 V was applied, and tests were carried out at potential scan rates from 5 to 1000 mV s^{-1}. For the RDE tests, a scan rate of 10 mV s^{-1} was fixed and the potential was sweep between the OCP and 0.6 V applying disc rotations from 100 to 2400 rpm. For the RRDE tests, a scan rate of 10 mV s^{-1} was also fixed and it was applied a rotation of 1200 rpm. In addition, the potential was scanned between the OCP and 0.6 V and the ring potential ranged between -0.9 and 0.25 V. All these three methods were carried out at room temperature (RT = 17 ºC) and 65 ºC. The LSV studies for hydrogen evolution reaction were made at 1 mV s^{-1} for 25 and 70 ºC from OCP to -2 V.

2.3 Electrolysis tests

The electrolysis tests were performed in a small-scale laboratory electrolyser (300 mL) using PAR 273A computer-controlled potentiostat/galvanostat (Princeton Applied Research, Inc.) and the associated PowerSUITE package to control the experiments. Gas quantification was done using a Ritter (MGC-1 V3.4 PMMQA) apparatus. Some electrolysis were made with nickel plates (A = 22.4 cm^2) as cathode and anode, other tests were carried out with nickel plate as the cathode and TiO_2-RuO_2 alloy as anode and, also the use of nickel plate as cathode and graphite as anode (A = 35.2 cm^2) was tested.
Besides the electrolysis tests, other tests using an anionic membrane (AMI-7001S), adding CO_2 bubbling into the electrolyte during electrolysis, and applying alternating current (AC) were studied, all with nickel electrodes.
Specifically, for AC electrolysis it was explored two different types of wave shape: half sinusoidal wave and pulsating waves. For both cases, the wave-shape and electrolysis parameters were verified on an oscilloscope (Tektronix TDS 1012B). For the first type of wave, an alternating power supply (230/12 V, 1 A) was used with a diode (ultra-fast rectifier BYV32) for rectification of the sinusoidal wave. For pulse generation a microcontroller based on Atmega328 processor was used and was developed a programmed code in C language to control the frequency and duty cycle of pulses.
The cell voltage applied in these studies were 1.5 V, 2.4 V, and 3 V and temperatures of 25, 50, 60, and 70 ºC were tested.

3 Results and discussion

3.1 Electrolyte characterisation

The results of conductivity, pH, density, and humidity content measurements are listed in Table 1.

Table 1 – Values of conductivity, pH, density, and humidity content for the prepared emulsion and waters from the liquefaction process.

	σ mS cm^{-1}	pH	ρ g dm^{-3}	humidity %
Emulsion	115	13.8	1123	78
Condensed water	8.73 x 10^{-3}	2.51	-	-
Light color phase	0.01 x 10^{-3}	1.53	-	-
Dark phase	11.2	2.09	-	-

3.2. Electrochemical studies

Cyclic Voltammetry

Cyclic voltammograms of emulsion 50/50 liquefied biomass + KOH (2 M) performed with Pt working electrode at 17 and 65 ºC are presented in Figure 1 and Figure 4, respectively.

Analysing Figure 1 the presence of two oxidation peaks, a_1 at -0.2 V and a_2 at 0.28 V, as well as one reduction peak, c_1 at -0.45 V can be verified. It is also notable that peak a_2 loses definition as the scan rate increases.

There are several hypotheses to explain the presence of these three peaks: it could correspond to (i) oxidation of two different species, being that one of them is later reduced; (ii) two-step oxidation of the same species that later is reduced; (iii) oxidation of one species that later suffers chemical reaction generating a different species that is oxidised corresponding to peak a_2 and then is reduced. Besides all these hypotheses, a more detailed study about peak c_1 is needed being that there is a possibility that this peak is independent of oxidation peaks (hypothesis justified with more detail further ahead). To analyse with more detail the behaviour of the system with scan rate it was represented three cyclic voltammograms at different scan rates (5, 50, and 200 mV s^{-1}).

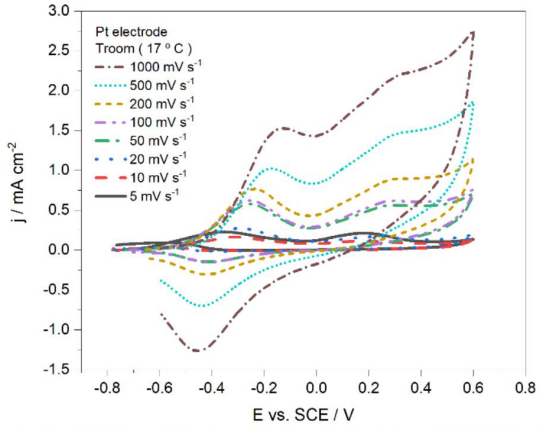

Figure 1 – Cyclic voltammograms of emulsion 50/50 liquefied biomass + KOH (2 M) using Pt working electrode and applying scan rates of 5 to 1000 mV s^{-1} at room temperature (17 ºC).

In Figure 2A at a low scan rate (5 mV s^{-1}) it is shown that besides the two oxidation peaks (a_1 and a_2) there is a third oxidation peak (c_2 at -0.6 V) in the backscan. This third anodic peak could be a consequence of the diffusional phenomenon. That is, after the second anodic peak (a_2), as the scan rate is so low, there is enough time for the oxidised species that were on the electrode's surface to diffuse to the bulk of the solution and, consequently, new species that are susceptible to oxidation can reach the electrode's surface. The disappearing of peak c_2 and the appearance of peak c_1 (Figure 2B,C) can be explained by the opposite way of thinking: after the second peak (a_2) at high scan rates, oxidised species don't have enough time to diffuse to the bulk of the solution, suffering reduction when more negative potentials are reached.

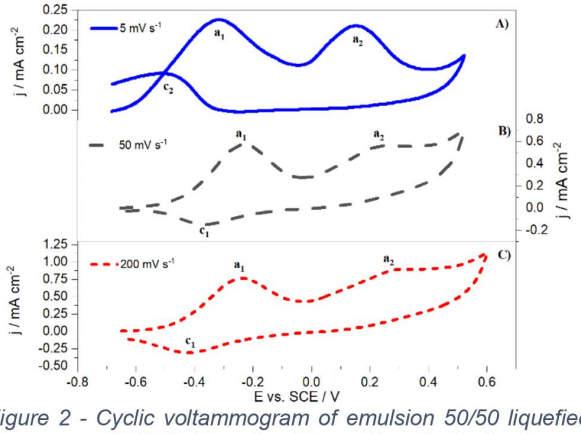

Figure 2 - Cyclic voltammogram of emulsion 50/50 liquefied biomass + KOH (2 M) using Pt working electrode at room temperature (17 ºC) with scan rates of A) 5 mV s^{-1}, B) 50 mV s^{-1} and C) 200 mV s^{-1}.

Going back to Figure 1, the presence of peak c_1 can indicate a possible reversible reaction. In other words, peak c_1 can correspond to the inverse process (reduction) of one of the anodic peaks a_1 or a_2 (oxidation). According to Pacheco *et al.* when a process is electrochemically reversible the anodic peak potential does not change with scan rate [12]. Thus, it would be intuitive to say that the oxidation process in peak a_2 would be reversible since its potential is always the same unlike peak a_1. However, according to the literature, reversibility depends on the scan rate, i.e., for sufficiently high scan rates all processes can appear irreversible [13]. Therefore, as at low scan rates (Figure 2A) the reduction peak (c_1) is not present is not possible to conclude that the oxidation process from peak a_2 is reversible and correspondent to peak c_1.

In order to exclude the hypothesis of peak a_1 being reversible, cyclic voltammograms at different scan rates were repeated but only until 0.1 V (Figure 3).

In Figure 3, it is possible to identify peak a_1 at -0.2 V, however, peak c_1 is not present. This fact reinforces the assumption of peak c_1 being independent of oxidation of the species from peak a_1.

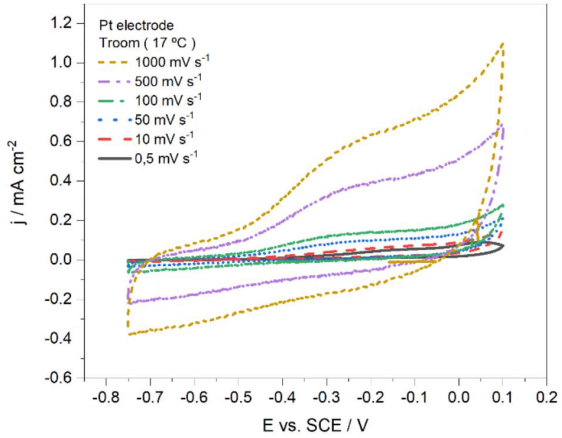

Figure 3 - Cyclic voltammograms of emulsion 50/50 liquefied biomass + KOH (2 M) using Pt working electrode and applying scan rates of 0.5 to 1000 mV s^{-1} at room temperature (17 ºC).

As there is no certainty about the reversibility of none of the peaks and that this concept depends on the scan rate, it was decided to apply the electrochemical equation for irreversible processes to calculate kinetic parameters. However, all these uncertainties are expected since according to Espinoza *et al.,* irreversibility is more prevalent than reversibility mainly in some redox pairs including organics [14]. Furthermore, Espinoza *et al.* also claim that oxidative or reductive degradation, dimerisation, reaction with solvent, fast mass transport and other processes that diminish the quantity of the species produced in the electrode's surface, have a strong influence on cyclic voltammograms causing asymmetries and even complete elimination of the anodic and cathodic peaks [14].

According to literature, the equation that represents oxidation and reduction peak's current dependency on scan rate for irreversible processes are equations (1 and (2, respectively,

$$i_p = 0{,}496\sqrt{(1-\alpha)n_a} \times nFAC\sqrt{\frac{FD\nu}{RT}} \qquad (1)$$

$$i_p = 0{,}496\sqrt{\alpha n_a} \times nFAC\sqrt{\frac{FD\nu}{RT}} \qquad (2)$$

where n is the number of exchanged electrons, F is the Faraday constant (96485 C mol^{-1}), A is the working electrode's area (0,1256 cm^{-2}), C is the concentration of electrochemically active species in the solution (3.34 x 10^{-5} mol cm^{-3}), D is the diffusion coefficient of that species (6.98 x 10^{-9} cm^2 s^{-1}), α is the charge transfer coefficient, n_a is the number of electrons involved in the rate-determining step (being 1 the most likely value), ν is the scan rate in V s^{-1}, R is the universal gas constant (8.314 J K^{-1} mol^{-1}) and T is the temperature in K.

To calculate the charge transfer coefficient for irreversible redox process Eqs. 3 and 4 were used and the results are in Table 2 [15,16].

$$E_p = \frac{RT}{2(1-\alpha)n_aF}\ln(\nu) + b \qquad (3)$$

$$E_p = -\frac{RT}{2\alpha n_aF}\ln(\nu) + b \qquad (4)$$

Table 2 - Kinetic parameters of redox processes using Pt working electrode at room temperature (17 ºC)

Kinetic parameters	Peak a_1	Peak a_2	Peak c_1
α	0.61	0.63	0.96
n	3.1	4.7	2.0

The charge transfer coefficient (α) is usually interpreted as being a measure of the position of transition state of the reaction, in this case, reduction reaction and, for oxidation reaction this coefficient is defined as 1-α. When α value is near 1 this implies the transition state is 'product-like' and similarly a value close to zero implies a 'reactant-like' transition state [17].

In order to study the influence of temperature another study with cyclic voltammograms was made at 65 ºC (Figure 4). In Figure 4 only one anodic peak (a_1) at -0.1 V can be seen and there is also a cathodic peak (c_1) at -0.4 V. The fact that there is only one anodic peak is probably due to the coalescence of peak a_1 and a_2 from Figure 1. Coalescence of peaks is due to similarity of values of potential of oxidation peaks at higher temperatures. Since the anodic peak has a similar potential to peak a_1 from Figure 1, is plausible that this peak is not influenced by temperature. Taking this hypothesis into account it is possible to claim that peak a_2 (from Figure 1) deviates to more negative potentials (towards peak a_1). This deviation indicates that at higher temperatures is easier to oxidise the species correspondent to peak a_2.

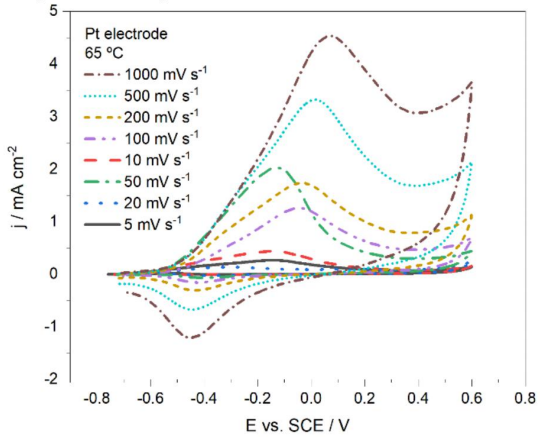

Figure 4 - Cyclic voltammograms of emulsion 50/50 liquefied biomass + KOH (2 M) using Pt working electrode and scan rates of 5 to 1000 mV s^{-1} at 65 ºC.

To study with more detailed the influence of scan rate in this system at 65 ºC cyclic voltammograms at 5, 50, and 200 mV s^{-1} were represented (Figure 5). It was found

that at 65 ºC the system has identical behaviour to the one verified at 17 ºC.
To calculate the kinetic parameters for the processes present in Figure 5 (Table 3) was used the already shown equations (Eqs. 1-4).

Table 3 - Kinetic parameters of redox processes using Pt working electrode at room temperature (65 ºC)

Kinetic parameters	Peak a_1	Peak c_1
α	0.57	0.93
n	4.6	1.0

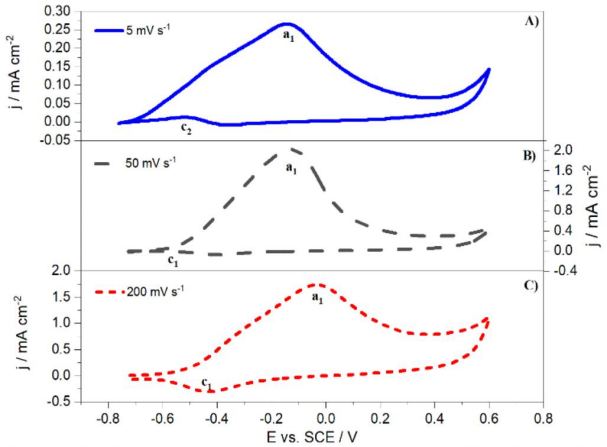

Figure 5 - Cyclic voltammograms of emulsion 50/50 liquefied biomass + KOH (2 M) using Pt working electrode at 65 ºC and applying scan rates of A) 5 mV s^{-1}, B) 50 mV s-1 and C) 200 mV s^{-1}.

In order to compare more clearly the difference between 17 and 65 ºC cyclic voltammograms at two different scan rates were represented in Figure 6.

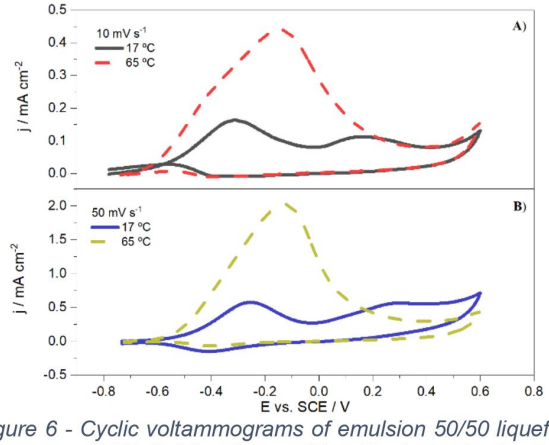

Figure 6 - Cyclic voltammograms of emulsion 50/50 liquefied biomass + KOH (2 M) using working Pt electrode. Study of variation of current density values with scan rates of A) 10 mV s^{-1} and B) 50 mV s^{-1} at 17 and 65 ºC.

In Figure 6, it is obvious that an increase in temperature increases current density, so, it is beneficial to carry out electrolysis at higher temperatures. Lastly, cyclic voltammograms of the emulsion 50/50 of liquefied biomass + KOH (2 M) before and after electrolysis (3 h) at different scan rates were represented in Figure 7. In this figure there are two events to be commented: a slight increase in current density of emulsion after electrolysis and a slight deviation of the oxidation peaks towards more positive potentials.
The first event is in accordance with previous studies with liquefied biomass (from cork) [18]. This can be explained by the fact that during electrolysis some organic compounds adsorb into the electrode's surface, hence, the electrolyte stays with a lower organic load, which increases the emulsion's conductivity.

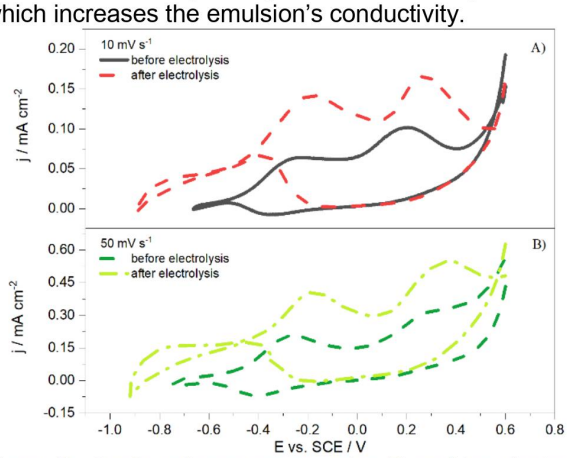

Figure 7 - Cyclic voltammograms using Pt working electrode of emulsion 50/50 of liquefied biomass + KOH (2 M) before and after electrolysis at A) 10 mV s^{-1} and B) 50 mV s^{-1}.

The second event was expected since after electrolysis the emulsion is more oxidised, therefore, is necessary to apply a higher potential to oxidise the remaining species. In Figure 7B appears a third oxidation peak in CV of the emulsion after electrolysis. This peak can be due to the increase of conductivity which indicates an increase of diffusion coefficient which in turn increases the transportation rate of new species to the electrode surface that are susceptible to oxidation.

3.2 Linear scan voltammetry – HER study

Hydrogen evolution reaction was studied through linear scan voltammetry (Figure 8) using Pt and Ni electrodes and applying Tafel's equation (eq. 5) to experimental data,

$$\eta = b \times \log(j) + a = \frac{2{,}3RT}{\alpha F}\log(-j) + \frac{2{,}3RT}{\alpha F}\log(-j_0) \qquad (5)$$

where η is the overpotential, j is the current density, α is the charge transfer coefficient, j_0 is the exchange current density (defined as the current density that flows equally in equilibrium and in both directions resulting in a zero net current and a zero net reaction rate [19]), F is the Faraday constant and R is the universal gas constant. LSV plots are presented in Figure 8. The corresponding

Tafel plots are in Figure 9 and the kinetic parameters obtained for both electrodes are in Table 4 and Table 5.

Table 4 - Tafel's kinetic parameters with Pt working electrode.

	25 ºC	70 ºC
b (mV dec^{-1})	284.0	319.5
α	0.21	0.21
j_0 (mA cm^{-2})	6.59 x 10^{-2}	1.58

Table 5 - Tafel's kinetic parameters with Ni working electrode.

	25 ºC	70 ºC
b (mV dec^{-1})	180.2	515.5
α	0.33	0.11
j_0 (mA cm^{-2})	6.30 x 10^{-2}	3.14

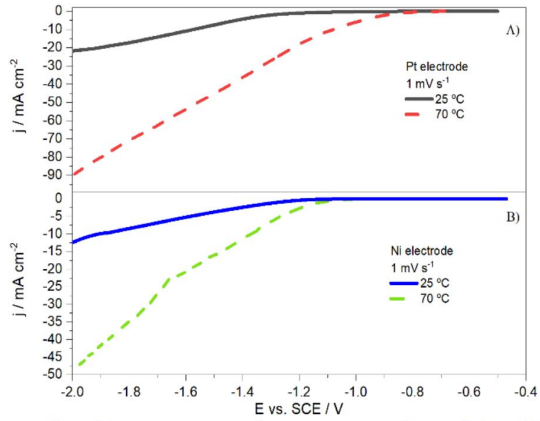

Figure 8 - Linear scan voltammogram of emulsion 50/50 liquefied biomass + KOH (2 M) to study of the cathodic zone using A) Pt working electrode and B) Ni working electrode at 25 and 70 ºC.

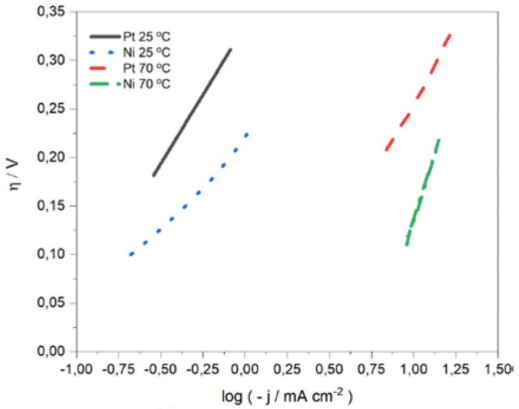

Figure 9 - j_p vs. $v^{1/2}$ (Tafel's plot) for Pt and Ni working electrodes at 25 and 70 ºC.

From Table 4 and Table 5 it can be verified that the increase in temperature increases the Tafel slope (b) and also j_0 value. According to literature, the values of Tafel slope with Pt electrode at 25 ºC for alkaline water and eucalyptus black liquor are 112.8 and 135.3 mV dec^{-1}, respectively, and j_0 values are 1.075 and 9.856 mA cm^{-2}, respectively [20]. Comparing these j_0 values to the ones obtained experimentally, it can be concluded that HER in these conditions (25 ºC and Pt electrode) using emulsion 50/50 liquefied biomass + KOH (2 M) is kinetically less favourable than in alkaline water and eucalyptus black liquor because j_0 obtained experimentally is much lower (6.59 x 10^{-2} mA cm^{-2}). However, j_0 increases (1.58 mA cm^{-2}) with temperature (70 ºC) reaching a value near alkaline water value. According to literature, the Tafel slope values with nickel electrodes vary between 200 and 1000 mV dec^{-1} due to the formation of nickel hydrides that limit the HER [21]. The values of Tafel slope from nickel electrodes tests for both temperatures are within this range. Analysing Tafel's slope values for all cases they are higher than 120 mV dec^{-1}, which means that HER in this system is limited by Volmer's step reaction, following alkaline water mechanism [20, 22].

3.3 Electrolysis

In this section, two different electrolysis modes were explored: direct current (DC) and alternating current (AC) electrolysis.

Direct current / Chronoamperometry

First, was made some tests to evaluate the most influencing variables in electrolysis that were possible to change. These variables are the composition of the anode material, the applied potential, and the temperature. This study is present in Figure 10 and Figure 11.

In Figure 10A is verified that an increase of 0.9 V increases current density from 0 to 0.6 mA cm^{-2} in stationary state. This result clarifies that despite of working at low potentials being always an advantage in terms of energetic costs, the increase in the potential to 2.4 V is beneficial to this electrolysis.

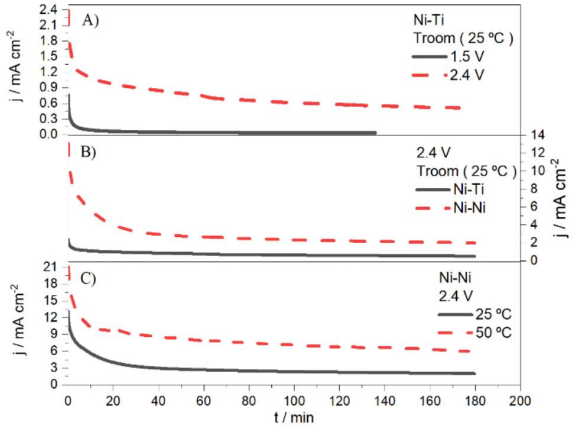

Figure 10 - Electrolysis studies with different operation conditions: A) Ni cathode and TiO_2-RuO_2 anode applying 1.5 and 2.4 V at 25 ºC, B) Ni electrodes applying 2.4 V at 25 and 50 ºC, C) Ni cathode and TiO_2-RuO_2 applying 2.4 V and 25 ºC.

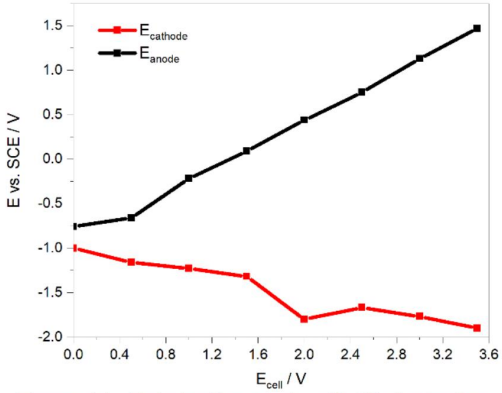

Figure 11 - Polarisation study with Ni electrodes.

Figure 10B evaluates temperature influence in electrolysis with Ni electrodes. In this graph is notable that when the temperature is duplicated from 25 to 50 ºC current density value (stationary state) increases more than double (from 2 to 7 mA cm^{-2}). Therefore, electrolysis at higher temperatures than 25 ºC is worth it. In order to make sure if Ni anode is better than TiO_2-RuO_2 anode for this electrolysis was made a test represented in Figure 10C. The results show that Ni generated higher current densities so it is the preferred one. Finally, a polarisation study was made to evaluate a possible optimum potential considering that one of the goals is to produce hydrogen. From Figure 11 it can be confirmed (also considering LSV studies) that to cathode polarisation reach -1.5 V is necessary to apply at least 2 V to the cell.

After this, study tests with Ni electrodes were carried out in order to optimise electrolysis. Thus, considering the results from Figure 10 and other tests that revealed that at 2.4 V and 25 ºC there was not any gas production it was decided to increase cell potential to 3 V and increase the temperature to 70 ºC (Figure 12).

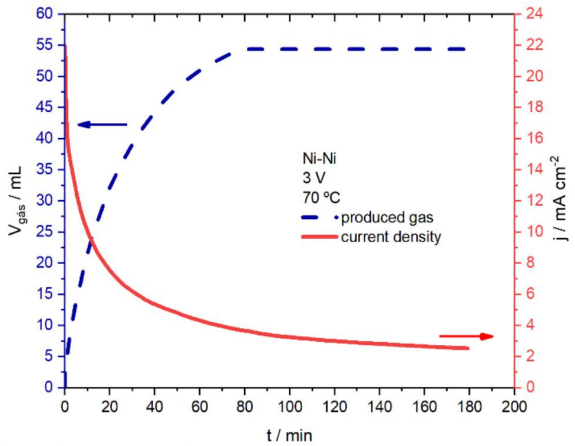

Figure 12 – Gas volume and current density generated in an electrolysis with Ni electrodes at 3 V and 70 ºC in 3 h.

From Figure 12 it can be seen that produced gas has the same behaviour as current density, i.e., there is gas production in the first 80 min until current density reaches stabilisation. When current density stabilises, the gas production stops. To make a more quantitative analysis of these results, faradaic (1st and 2nd Faraday's law – eq. 6 and 7) and energetic efficiency (eq. (8) were calculated (Table 6) considering that all gas produced is hydrogen,

$$1^{st}\ \text{Faraday law} \quad Q = i \times t \tag{6}$$

$$2^{nd}\ \text{Faraday law} \quad m_{H_2} = \frac{Q \times MM}{F \times n} \tag{7}$$

where Q is the charge in A s, i is the current in A, t is time in s, m_{H_2} is the produced hydrogen mass in g, MM is the molecular weight of H_2 (2.02 g mol^{-1}), F is the Faraday constant and n is the number of changed electrons (in this case, n=2).

$$\eta_{energy} = \frac{n_{\dot{H}_2} \times HHV_{H_2}}{\dot{W}_e} \tag{8}$$

where, $n_{\dot{H}_2}$ is the produced hydrogen flow in mol s^{-1}, HHV_{H2} is the high heating value of hydrogen in kJ mol^{-1} (286.6 kJ mol^{-1}) and $\dot{W}_e$ is the energy given to the system in kW.

This test was the one with higher efficiency values. The Faradaic and energetic efficiency where 43 and 38.5 %, respectively.

An electrolysis with Ni electrodes applying 3 V at 60 ºC using an anionic membrane (AMI-7001S) was tested. From this test, it was clear that there is only production of gas on the cathode side, which means that this gas is very likely to be hydrogen. This statement is corroborated by a study by A. Caravaca *et al.* that concludes that organic matter oxidation, more specifically lignin, happens at a lower potential than water oxidation, therefore, O_2 production does not happen [23] This electrolysis test served mostly for observation of gas production side as in terms of current density did not show any improvement and it has the risk of obstruction.

As one of the goals of this work was to study CO_2 incorporation in electrolysis, some tests were made with Ni electrodes applying 3 V and bubbling CO_2 (Figure 13).

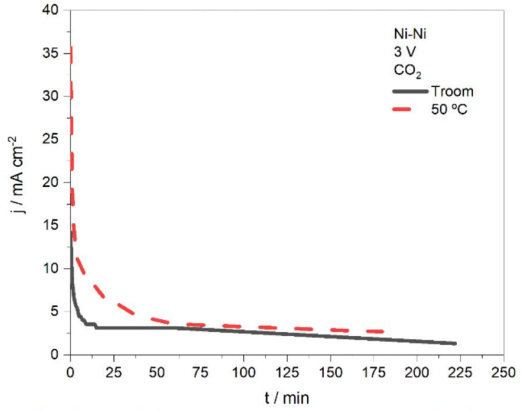

Figure 13 - Current density from electrolysis with Ni electrodes, bubbling CO_2 and applying 3 V at RT and 50 ºC.

From Figure 13 results it is clear that in these operating conditions the influence of temperature on current density is despicable and its values do not show any improvement.

Alternating current

Since literature claims that using an alternating current power supply can disturb the diffusion layer, some tests with this current mode were made [24]. For these tests, a half sinusoidal wave was applied to avoid electrode's polarity inversion to ensure that ions move only in one direction. So, the potential varied between 0 and a maximum of 3 V (in this case). It should be noted that within this section, when applied potential is referred it corresponds to the RMS value. The results showed that the current density generated was not much different from DC tests. Thus, is possible that electrolysis is still limited by diffusion.

Since half-wave application did not produce improved results it was decided to apply pulses instead. It is proved that pulses in electrolysis prevent diffusion layer formation since the current is interrupted before this layer is fully developed. Therefore, studies claim that this phenomenon decreases cell overpotential [24].

The pulse characteristics used are: 3 V, 300 Hz and a peak-to-peak value of 4 V. To have a more clear understanding of optimum conditions for electrolysis various tests with different operating conditions were chosen and represented in Figure 14.

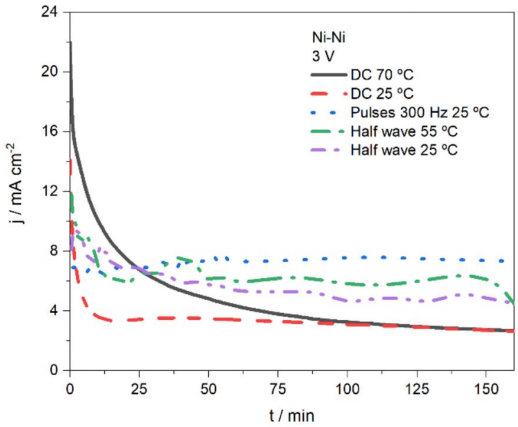

Figure 14 - Current densities from electrolysis with Ni electrodes, applying 3V and: DC at 25 and 70 ºC, AC with half wave at 25 and 55 ºC and pulses with 300 Hz at 25 ºC.

From Figure 14 it is notable that pulsed electrolysis generates more stable current densities and after 30 min these currents are even higher than all the other tests. Still, the quantity of gas produced was only the minimum detected by the device (3.2 mL).

Another test was made bubbling CO_2 with pulsed electrolysis. The result was represented along with a test without CO_2 bubbling to compare the system performance (Figure 15). This test showed that electrolysis without CO_2 generates more stable current densities than with CO_2.

Because of low produced gas quantities in pulsed electrolysis from Figure 14, it was decided to increase peak-to-peak value to 7 V, keeping the same RMS value and, since pulses shape was deforming through time, the circuit was changed in order to impose a discharge of diffusion layer when the potential is 0 V. Results from these changes are presented in Figure 16 and Table 6.

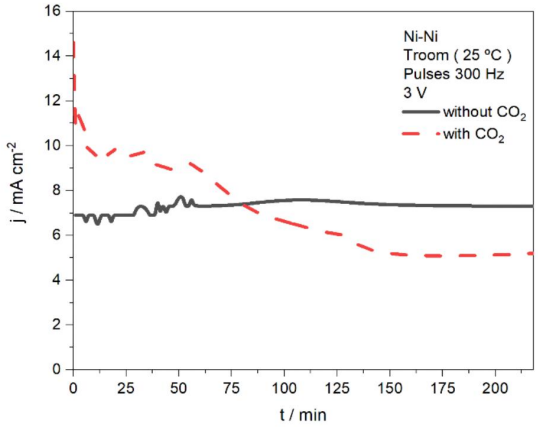

Figure 15 - Current density from pulsed electrolysis with Ni electrodes at room temperature, 3V and 300 Hz with and without CO_2 bubbling.

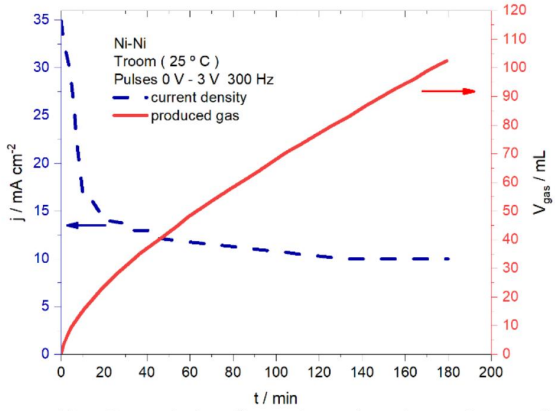

Figure 16 - Current density and produced gas from pulsed electrolysis with Ni electrodes imposing a moment of 0 V and at 300 Hz and room temperature.

Table 6 – Information about electrolysis performance with Ni electrodes at 3 V for 3 h, with direct current at 70 ºC, and applying pulses (300 Hz) at room temperature: theoretical hydrogen production, experimentally produced gas, Faradaic, and energetic efficiency.

Tests	Theoretical H_2 / mL	Produced gas / mL	$\eta_{Faradaic}$ / %	$\eta_{energetic}$ / %
DC	127	55	43	38.5
Pulses	343.3	102.4	29.8	10.8

This test (Figure 16) was the one that generated higher current density (stabilisation value of 10 mA cm^{-2}) and produced more quantity of gas (102.4 mL). However, the Faradaic and energetic efficiency are low (29.8 and 10.8%, respectively).
Results from Table 6 show a promising electrolysis, however, still in need of optimisation of the operating conditions to increase both faradaic and energetic efficiency.

Tests with waters from liquefaction process

In order to reuse waters from the liquefaction process, some emulsions were prepared to evaluate its performance on electrolysis. These emulsions were constituted by 50 % of liquefied biomass and 50 % of water (condensed water and dark phase from the liquefaction process (% v/v)). The light colour phase water had a null electrochemical activity so it was not used for further tests. Since the emulsion conductivity would be very low was necessary to add 1 mL H_2SO_4 50% (m/m) to increase this parameter. The results are present in Figure 17 along with a test with emulsion liquefied biomass + KOH (2 M) to compare.
Figure 17 shows that current density from electrolysis with waters from the liquefaction process are higher than alkaline emulsion, however, stabilisation values are not very distant from each other. Despite the good results with water from the liquefaction process, a higher anode mass loss was found in these tests compared to the alkaline emulsion. Thus, to evaluate whether this approach is worth it, produced gas should be measured to calculate faradaic and energetic efficiencies.

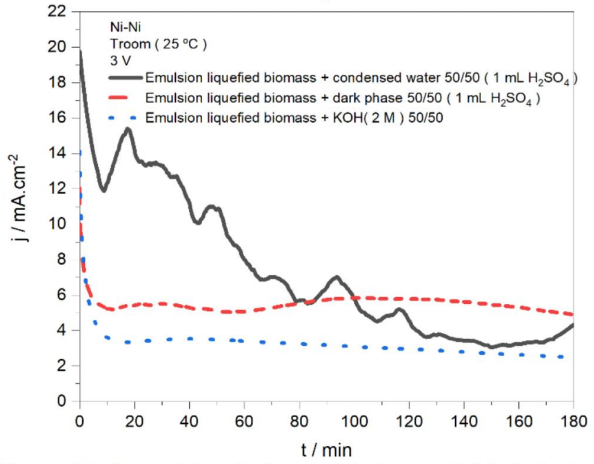

Figure 17 - Current density from electrolysis with Ni electrodes applying 3V at room temperature with different emulsions 50/50: liquefied biomass + condensed water/ dark phase/ KOH (2M).

4 Conclusions

In this study, optimisation of electrolysis of liquefied biomass to produce hydrogen, produce value-added compounds through oxidation of organic matter and CO_2 capture into electrolysis were the main goals. Since there is low information about the electrochemical activity of liquefied biomass (and consequently about the prepared emulsion) some electrochemical studies were made. These studies included cyclic voltammetry and LSV.
From cyclic voltammetry, it was verified that organic matter from liquefied biomass is susceptible to redox reactions. Comparing CVs from emulsion before and after electrolysis, an increase in current density, a deviation of peaks towards more positive potentials, and the presence of a 3rd anodic peak were observed. The first observation indicates is due to the loss of some organic compounds that adsorb into the electrodes, the second indicates that the emulsion after electrolysis is more oxidised and, the third one is due to an increase of emulsion's conductivity. The hydrogen evolution reaction study concluded that this reaction in Pt electrode is kinetically harder than in water and black liquor.
Electrolysis preliminary tests with direct current showed that a potential higher than 2 V is needed and is beneficial in terms of current density, Ni electrodes are better than Ti alloy electrodes and a temperature higher than room temperature is also beneficial.
The best result from direct current tests was applying 3 V and 70 ºC with Ni electrodes where a 38.5 % energetic efficiency and a 43 % faradaic efficiency were obtained.
The electrolysis test that produced more gas was the one with pulsed current with 300 Hz at 3 V and room temperature. This test had 10.8 % of energetic efficiency and 29.8 % faradaic efficiency.
Electrolysis tests bubbling CO_2 showed no improvement either with direct current or alternating current in terms of current density values.
The incorporation of waters from the liquefaction process showed an increase of current density during electrolysis, however, an increased electrode mass loss was verified.
This work shows a promising way to produce H_2 without O_2 contamination, nevertheless, it still needs optimisation of operating conditions and a more profound study to certificate if high-value compounds are being formed due to the oxidation of organic matter and if CO_2 bubbling can contribute to the formation of other valuable gases.

Acknowledgments

This work was carried out under the Project Clean4G POCI-01-0247-FEDER-038323 funded by Portugal 2020 through European Regional Development Fund (ERDF) in the frame of COMPETE 2020.

References

1. Mckendry P (2002) Energy production from biomass (part 1): overview of biomass. Bioresource Technology 83: 37-46.

https://doi.org/10.1016/S0960-8524(01)00118-3
2. Brandt A, Gräsvik J, Hallett JP, Welton T (2013) Deconstruction of lignocellulosic biomass with ionic liquids. Green Chemistry 15:550–583. https://doi.org/10.1039/C2GC36364J
3. Nabgan W, Tuan Abdullah TA, Mat R, Nabgan B, Gambo Y, Ibrahim M, Ahmad A, Jalil A, Triwahyono S, Saeh I (2017) Renewable hydrogen production from bio-oil derivative via catalytic steam reforming: An overview. Renewable and Sustainable Energy Reviews 79:347–357. https://doi.org/10.1016/j.rser.2017.05.069
4. Carvalho R, Mateus MM, Galhano R, Santos D Cork Liquefaction: Improvement of the Process and its Application on Adhesives Formulation (Master Thesis, Universidade de Lisboa, Lisbon, Portugal)
5. Akhtar J, Amin NAS (2011) A review on process conditions for optimum bio-oil yield in hydrothermal liquefaction of biomass. Renewable and Sustainable Energy Reviews 15:1615–1624. https://doi.org/10.1016/j.rser.2010.11.054
6. Kim JY, Lee HW, Lee SM, Jae J, Park Y (2019) Overview of the recent advances in lignocellulose liquefaction for producing biofuels, bio-based materials and chemicals. Bioresource Technology 279:373–384. https://doi.org/10.1016/j.biortech.2019.01.055
7. Zhang X, Chan SH, Ho HK, Tan S, Li M, Li G, Li J, Feng Z (2015) Towards a smart energy network: The roles of fuel/electrolysis cells and technological perspectives. International Journal of Hydrogen Energy 40:6866–6919. https://doi.org/10.1016/j.ijhydene.2015.03.133
8. Chi J, Yu H (2018) Water electrolysis based on renewable energy for hydrogen production. Cuihua Xuebao/Chinese Journal of Catalysis 39:390–394. https://doi.org/10.1016/S1872-2067(17)62949-8
9. Zhang Y, Guo SX, Zhang X, Bond A, Zhang J (2020) Mechanistic understanding of the electrocatalytic CO2 reduction reaction – New developments based on advanced instrumental techniques. Nano Today 31:100835. https://doi.org/10.1016/j.nantod.2019.100835
10. Liang S., Altaf N., Huang L., Gao Y, Wang Q (2020) Electrolytic cell design for electrochemical CO_2 reduction. Journal of CO_2 Utilization 35:90–105. https://doi.org/10.1016/j.jcou.2019.09.007
11. Guerra L, Moura K, Rodrigues J, Gomes J, Puna J, Bordado J, Santos T (2018) Synthesis gas production from water electrolysis, using the Electrocracking concept. Journal of Environmental Chemical Engineering 6:604–609. https://doi.org/10.1016/j.jece.2017.11.033
12. Pacheco WF, Semaan FS, Almeida VGK, Ritta A, Aucélio R (2013) Voltammetry: A brief review about concepts. Revista Virtual de Quimica 5:516–537. https://doi.org/10.5935/1984-6835.20130040
13. Elgrishi N, Rountree KJ, McCarthy BD, Rountree E, Eisenhart t, Dempsey J (2018) A Practical Beginner's Guide to Cyclic Voltammetry. Journal of Chemical Education 95:197–206. https://doi.org/10.1021/acs.jchemed.7b00361
14. Espinoza EM, Clark JA, Soliman J, Derr J, Morales, Vullev V (2019) Practical Aspects of Cyclic Voltammetry: How to Estimate Reduction Potentials When Irreversibility Prevails. Journal of The Electrochemical Society 166:H3175–H3187. https://doi.org/10.1149/2.0241905jes
15. Santos DMF, Sequeira CAC (2010) Cyclic voltammetry investigation of borohydride oxidation at a gold electrode. Electrochimica Acta 55:6775–6781. https://doi.org/10.1016/j.electacta.2010.05.091
16. Cardoso DSP, Santos DMF, Šljukić B, Sequeira C, Macciò D, Saccone A (2016) Platinum-rare earth cathodes for direct borohydride-peroxide fuel cells. Journal of Power Sources 307:251–258. https://doi.org/10.1016/j.jpowsour.2015.12.131
17. Danlei Li, Chuhong Lin, Christopher Batchelor-McAuley, Lifu C, Richard C (2008) Tafel analysis in practice. Journal of Electroanalytical Chemistry 826:117-124. https://doi.org/10.1016/j.jelechem.2018.08.018
18. Silva T (2018) Electrochemical Conversion of Liquefied Forest Biomass (Master Thesis, Instituto Superior Técnico, Lisbon, Portugal)
19. Bard AJ, Faulkner LR (2001) Electrochemical Methods, Second Edition, John Wiley & Sons, Inc., Texas, United States
20. Ghatak HR, Kumar S, Kundu PP (2008) Electrode processes in black liquor electrolysis and their significance for hydrogen production. International Journal of Hydrogen Energy 33:2904–2911. https://doi.org/10.1016/j.ijhydene.2008.03.051
21. Shinagawa T, Garcia-Esparza AT, Takanabe K (2015) Insight on Tafel slopes from a microkinetic analysis of aqueous electrocatalysis for energy conversion. Scientific Reports 5: 13801. https://doi.org/10.1038/srep13801
22. Caravaca A, Garcia-Lorefice WE, Gil S, Lucas-Consuegra A, Vernoux P (2019) Towards a sustainable technology for H 2 production: Direct lignin electrolysis in a continuous-flow Polymer Electrolyte Membrane reactor. Electrochemistry Communications 100:43–47. https://doi.org/10.1016/j.elecom.2019.01.016
23. Vincent I, Choi B, Nakoji M, Ishizuka M, Tsutsumi K, Tsutsumi A (2018) Pulsed current water splitting electrochemical cycle for hydrogen production. International Journal of Hydrogen Energy 43:10240–10248. https://doi.org/10.1016/j.ijhydene.2018.04.087